

Spark Ignition Characteristics of a LO₂/LCH₄ Engine at Altitude Conditions

Julie Kleinhenz¹, Charles Sarmiento², and William Marshall³
NASA Glenn Research Center, Cleveland, OH, 44135

The use of non-toxic propellants in future exploration vehicles would enable safer, more cost effective mission scenarios. One promising “green” alternative to existing hypergols is liquid methane/liquid oxygen. To demonstrate performance and prove feasibility of this propellant combination, a 100lb_f LO₂/LCH₄ engine was developed and tested under the NASA Propulsion and Cryogenic Advanced Development (PCAD) project. Since high ignition energy is a perceived drawback of this propellant combination, a test program was performed to explore ignition performance and reliability versus delivered spark energy. The sensitivity of ignition to spark timing and repetition rate was also examined. Three different exciter units were used with the engine’s augmented (torch) igniter. Propellant temperature was also varied within the liquid range. Captured waveforms indicated spark behavior in hot fire conditions was inconsistent compared to the well-behaved dry sparks (in quiescent, room air). The escalating pressure and flow environment increases spark impedance and may at some point compromise an exciter’s ability to deliver a spark. Reduced spark energies of these sparks result in more erratic ignitions and adversely affect ignition probability. The timing of the sparks relative to the pressure/flow conditions also impacted the probability of ignition. Sparks occurring early in the flow could trigger ignition with energies as low as 1-6mJ, though multiple, similarly timed sparks of 55-75mJ were required for reliable ignition. An optimum time interval for spark application and ignition coincided with propellant introduction to the igniter and engine. Shifts of ignition timing were manifested by changes in the characteristics of the resulting ignition.

Nomenclature

ACS	=	Altitude Combustion Stand
BDV	=	Breakdown Voltage
DSO	=	Digital Storage Oscilloscope
E _{spark}	=	Energy of the spark discharge, milliJoules
HV	=	High Voltage
I	=	Current, Amps
I-bit	=	Impulse Bit
I _{sp}	=	Specific Impulse
LCH ₄	=	Liquid Methane
LO ₂	=	Liquid Oxygen
PCAD	=	Propulsion and Cryogenic Advanced Development Project
PLC	=	Programmable Logic Controller
RCE	=	Reaction Control Engine
V	=	Voltage, Volts
Vdc	=	Volts from Direct Current
VEE	=	Variable Energy Exciter

¹ Research Engineer, Propulsion and Propellants Branch, 21000 Brookpark Rd MS 301-3, Senior Member.

² Aerospace Engineer, Space Propulsion Branch, 21000 Brookpark Rd MS 86-8, Non-member.

³ Research Engineer, Propulsion and Propellants Branch, 21000 Brookpark Rd MS 301-3, Senior Member.

I. Introduction

The next generation of chemical propulsion systems will enable exploration missions beyond earth orbit. Cryogenic bi-propellants are attractive for their high performance. Traditionally hydrogen has been favored as the fuel, but its thermal storage requirements (low boiling point) create additional vehicle dry mass, reducing potential payload capacity. Hypergolic propellants, such as hydrazine, are a common alternative but are highly toxic. The rigid handling and containment procedures are not cost efficient. Hydrocarbon fuels, methane in particular, are appealing for their high performance potential (when paired with oxygen) and moderate thermal storage requirements. This combination is also non-toxic, enabling simpler handling and storage methods. Methane can be produced from local resources on some exploration destinations, such as Mars.

Prior work with this propellant combination is limited, so a goal of the NASA Propulsion and Cryogenic Advanced Development (PCAD) project was to examine the feasibility and performance characteristics of these non-toxic propellant systems¹⁻³. As part of this project, a 100 lb_f Reaction Control engine (RCE) was developed by Aerojet Corporation to study liquid oxygen/liquid methane (LO₂/LCH₄) combustion⁴, and was tested at altitude conditions using the Altitude Combustion Stand at NASA Glenn Research Center during 2009 and 2010 (Fig. 1). In particular, there was interest in demonstrating repeatable and reliable ignition of the engine for a wide range of propellant inlet temperatures.

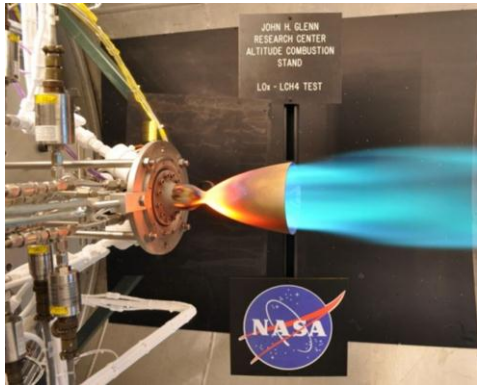


Figure 1: The 100 lb_f RCE operating at altitude conditions in the ACS facility.

The first series of tests^{5,6} explored the Specific Impulse (I_{sp}) performance with burn times up to 7 s. The engine met its I_{sp} goal, and demonstrated improved performance as propellant temperature increased or as mixture ratio decreased, which is consistent with previous studies. The next test series examined the Impulse Bit (I-bit) performance for pulsed mode operation⁷. Again, the engine met its goals, achieving I-bits <4 lbf-s with pulse durations under 80 ms. As many as 30 consecutive pulses at a 5 percent duty cycle were repeatedly achieved.

In the final test series, which will be discussed in this document, ignition characteristics were examined for engine hot fires at altitude conditions. Since one of the perceived drawbacks of this propellant combination is the anticipated need of higher ignition energy (relative to oxygen/hydrogen), the goal was to explore ignition performance and reliability versus delivered spark energy. An augmented, or spark torch, igniter configuration was used in this engine to enable better control of the spark environment (versus a direct spark ignition within the main chamber), as demonstrated in previous oxygen/hydrocarbon engine designs^{8,9}. Based on this previous engine work, it was expected that 40-50 mJ sparks would be required to obtain reliable ignition of the oxygen/methane propellants. A variable energy exciter unit was developed in-house to explore the ignition energy limits. Exciters used in the previous I_{sp} and I-bit test series were also tested in order to help interpret the ignition behaviors observed in those tests. All of the exciter units were instrumented to obtain high fidelity spark current and voltage waveform information. By coupling such data to the pressure and flow measurements in the engine, it was possible to identify the ignition spark in terms of energy and timing. This document summarizes the findings of the study, but detailed results can be found in Ref. 10.

II. Experimental Setup

A. Hardware

All ignition tests were performed using the Aerojet 100 lb_f RCE⁴. This radiative cooled 45:1 columbium nozzle was designed to operate at a nominal mixture ratio of 2.5 and a chamber pressure of 175 psia. The details of the configuration are described in detail in Ref. 5. With the exception of exciter units, the tested engine configuration remained unchanged throughout all of the PCAD test series.

The engine is designed for use with an augmented, or spark torch, igniter and capacitive discharge exciter. Ignition therefore consists of lighting the spark torch which then ignites the main chamber. Unlike traditional augmented ignition systems, propellant flow to the igniter in this engine was integrated into the main feed system and not independently controlled. Therefore, ignition tests necessarily involved a main chamber burn. Approximately 2.5 percent of the total propellant flow to the engine was directed to the igniter cavity, where the nominal mixture ratio was approximately 1.82.

All tests took place at altitude conditions in the NASA Glenn Research Center's Altitude Combustion Stand (ACS). The facility can accommodate a 2000 lbf class engine with chamber pressure up to 1000 psia, using liquid and gaseous oxygen, liquid and gaseous hydrogen, liquid methane, or other hydrocarbon propellants. To accommodate the propellant temperature control needed in this investigation, the standard feed system was replaced with two propellant conditioning feed systems. Over 100 data channels are dedicated to the research hardware alone and logged at 1000 Hz. All system timing is controlled using a Programmable Logic Controller (PLC) which has a 10 ms resolution.

Three exciter units were used in the course of this test program, however only the results of two units will be presented here. The first unit, called the Variable Energy Exciter (VEE), was developed in-house to permit energy and spark rate variation. The second unit, a Unison exciter, had been used during the I-bit test program. The final unit, a Champion exciter, was used for the I_{sp} performance test series, but will not be covered in these discussions. The bipolar sparks of this exciter required high data acquisition rate to resolve the polarity shifts. Using the available data system, it was only possible to capture a single spark in the train, with no guarantee that it would be the ignition spark. Thus only a limited data set was obtained with the Champion exciter, but these results are included in Ref. 10. On the whole, the three exciters provided a good mix of exciter types and capabilities, so all three are included for comparison in Table 1. Note that the Champion and Unison were chosen based on availability and convenience, and the results presented here should not be construed as an endorsement of these units.

The same spark plug was used with all exciters. It featured a button tipped electrode with a 0.64 mm igniter annular spark gap. It was connected to the exciters using a 3.65 m, unshielded, silicone insulated, and atmosphere sleeved ignition cable. Cable shielding was eliminated to facilitate insertion of diagnostic probes and to avoid its added capacitive load on the exciter output. Despite also minimizing cable length for the test arrangement, the remaining capacitive load of the long cable still significantly attenuated the high voltage pulse delivered to the igniter spark gap. The spark current return path was provided by the facility ground structure.

All units were instrumented with voltage and current probes, which were located on the ignition cable near the exciter. These probes were not vacuum compatible, so the exciters were located outside the vacuum vessel. The high voltage ignition cable penetrated the vessel within a pressurized sleeve to prevent corona discharge. The voltage and current data were captured by a digital storage oscilloscope (DSO) for high speed waveform data acquisition.

Table 1: Specifications of the three exciters used in the Ignition Margin program.

	VEE	Unison	Champion
Type	Uni-polar	Uni-polar	Bi-polar
Spark Rate, sparks/sec	Variable, 125 to 250	200	100
Delivered Spark Energy*, mJ	30 to 50	55 to 65	12
Spark discharge time, μ s	100 to 400	200	50
Time to first spark, ms	21	6.5	3 to 9
Delivered High Voltage Pulse**, kV	9 to 10	5 to 6	5 to 6

* As measured for quiescent air spark gap.

** High voltage pulse measured after cable attenuation

B. Test Procedure

Ideally, the engine would be fired in pulsed operation mode, where multiple ignition opportunities would be possible per test. However, the data from the digital oscilloscope could not be output to memory quickly enough to permit this. Therefore each ignition test was a single engine cycle. Typically 10 tests could be performed in one day, though as many as 23 were possible depending on the test matrix. Once ignited, the burn duration was 1 s at a simulated altitude of 75,000 - 120,000 ft (0.2 - 0.5 psia).

Timing of exciter and flow command signals was constrained by the facility PLC to 10 ms steps. As with the previous test series^{5,7}, the LO_2 flow was initiated first, with LCH_4 flow initiation 10 ms later. In the previous I_{sp} and I-bit test series, the exciter was always initiated prior to propellant flow (10 ms before the LO_2 valve command). This timing was varied in the test series to help identify the igniting spark within the spark train and to explore different ignition behaviors.

Historically, spark ignition systems have been operated using spark trains, which is a series of sparks triggered over a specified time. This is done to ruggedize the system against variations in propellant flow. The presence of a flow field, especially a turbulent one, can reduce ignition probability for a single spark¹¹. For most of these tests, the exciter was active for 60 ms, where the number of sparks occurring in that time varied depending on the spark rate of the exciter.

While exciter settings were varied according to each exciter’s capabilities, the engine conditions were kept constant. The pressures in the run tank govern mixture ratio and were set to achieve a mixture ratio of 2.5 at steady state conditions. (The flow conditions were still transient during the ignition time span). During tests with the Unison exciter, propellant temperature (measured at the fire valve) was varied among the previously established setpoint conditions; cold (170 °R LCH₄, 163 °R LO₂), nominal (204 °R), and warm (224 °R). For the other two exciters, only nominal temperature conditions were used.

A total of 87 runs were performed during this test program using the three exciter units. The VEE was used in 28 hot fire tests over the course of 2 days. During the first day, only the energy setpoint was varied, while both energy and spark rate were varied the second day. The Unison exciter was tested for 3 days, using a different propellant temperature each day. A total of 44 hot fire tests were performed with spark command timing varied within each test day. The Champion exciter was tested for just 1 day, with 15 hot fire tests (results in Ref. 10). Since only 1-2 sparks could be captured within the data resolution of the oscilloscope, the oscilloscope timing was the sole variable in those tests.

C. Data Reduction Method

Spark energies were calculated using the discharge voltage and current data from the digital oscilloscope. Figure 2 shows an example waveform for a single spark from the Unison exciter. (A VEE waveform was similar). The discharge voltage (circles) and current (triangles) waveforms for a single spark are shown at the bottom. A spark discharge is indicated when the current signal rises above its zero level (the unfiltered signal resulted in a zero offset). Energy was determined by calculating and then integrating the power level during this period, as shown in Equation 1 (where V is Voltage, I is current, and t is time).

$$\text{Equation 1} \quad E_{spark} = \int |V * I| dt$$

The squares at the top of Fig. 2 show the power calculation for each time step and the shaded region indicates the integration time. The energy for this spark was 63mJ.

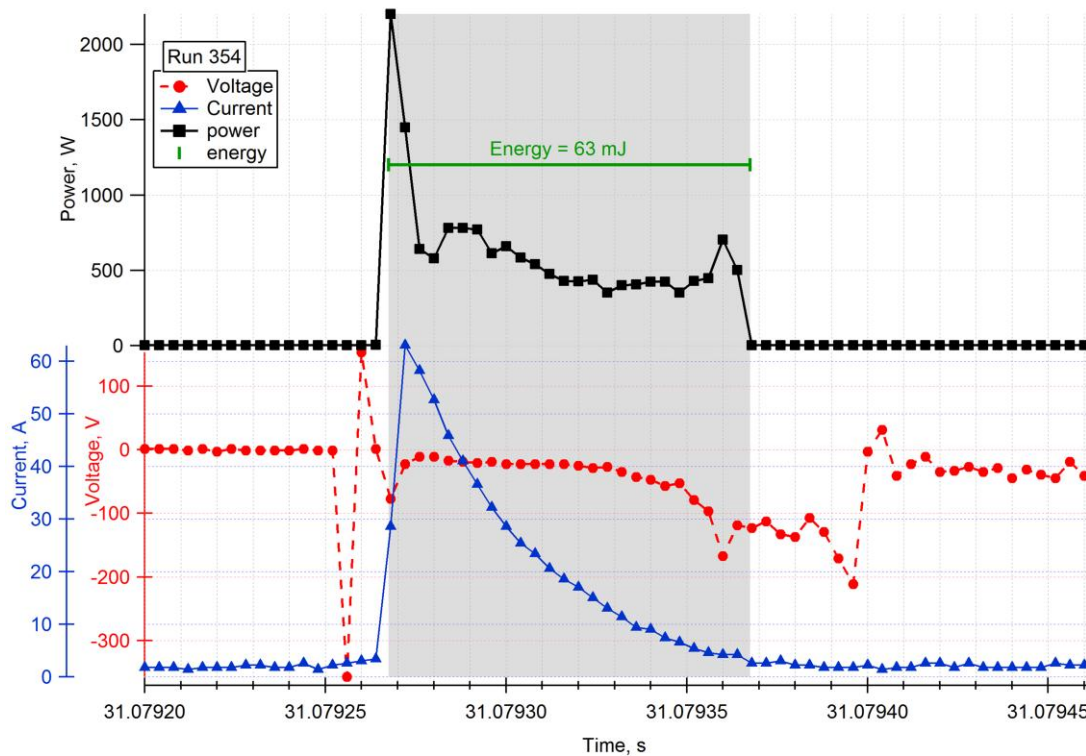


Figure 2: An example energy calculation is shown. The voltage and current of a single spark is shown at the bottom, with the power at the top. Energy is calculated by integrating the power curve during the time the current exceeds its noise floor, represented by the highlighted region.

Determining ignition energy required identifying which spark triggered ignition. This was particularly important since the delivered spark energies varied within a spark train. Ignition was indicated by a rise in pressure in both the igniter cavity and the engine chamber. The spark waveform data was synchronized with the engine pressure data to determine ignition. Figure 3 shows an example of the overlaid data. The sparks are indicated by spikes in the voltage and current signals (lower left axis), and the energy levels of each spark are indicated at the top. The dashed lines indicate the initiation of the propellant flow based on manifold pressures; at ~ 31.074 s for LO_2 and ~ 31.084 s for LCH_4 . The squares and circles denote the chamber and igniter cavity pressures, respectively, while the open symbols show cold flow pressures for comparison. Ignition occurs when the igniter and chamber pressures deviate from the cold flow values. This example shows a test with the VEE using a low spark rate (the VEE is the only unit that permitted spark rate variation). The pressure response indicates ignition at 31.085s, between the first and second sparks. Thus, it was the first spark that triggered the ignition, but the pressure response lagged the spark by about 4 ms. Another indicator is the temperature in the igniter cavity, represented by the solid line, which begins to rise about 8 - 10 ms after the ignition spark. These delay times are corroborated by other tests with the VEE at varying spark rates as well as a Unison test with a shortened spark command time.

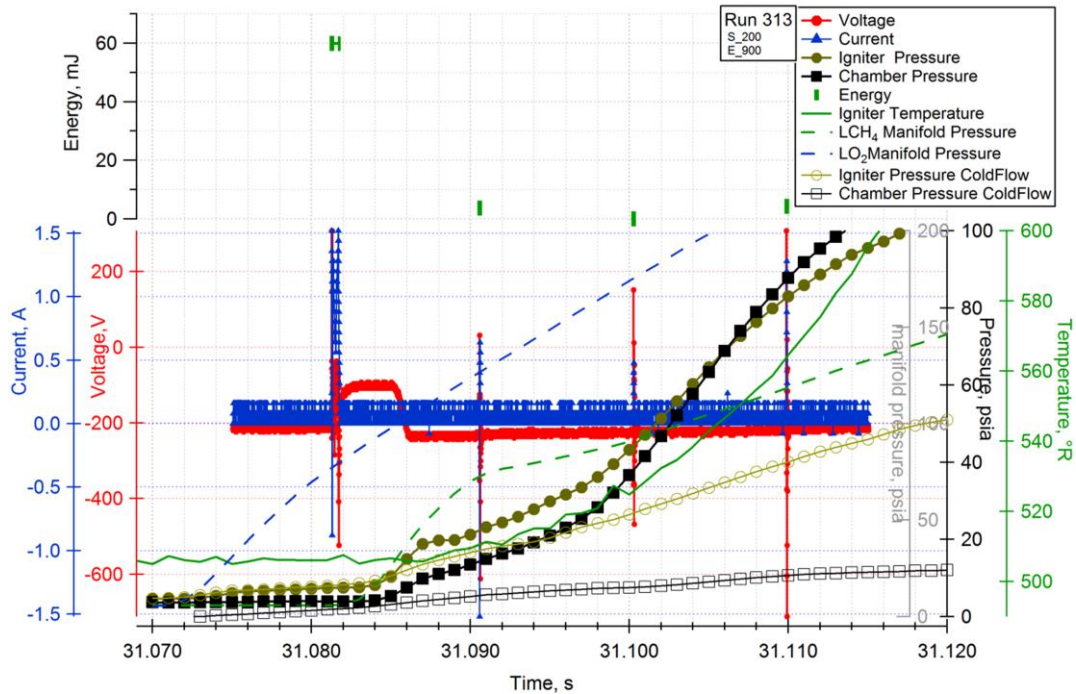


Figure 3: An example data set taken from the VEE with a low spark rate. The pressures rise occurs between the first and second sparks, so the first spark must have triggered the ignition. The pressure response is delayed by ~ 4 ms relative to the ignition spark and igniter cavity temperature has an 8-10 ms delay.

III. Results

The following sections explore several different aspects that affect ignition. The flow field of the hot fire environment has a significant effect on ignition behavior. Thus, the results focus not only on energy, but on ignition timing relative to initiation and ramp up of the propellant flow.

A. Engine Environment

The igniters were all tested in room conditions prior to the hot fire tests. These “dry sparks” occurred in air at room pressure conditions with no propellant flow. Figures 4 and 5 shows comparisons of hot fire spark waveforms (a) and dry sparks (b) for the Unison exciter. Figure 4 shows the full spark trains relative to the flow conditions (using the same convention as in Fig. 3). Figure 5 shows the corresponding close up views of each individual spark waveform. The dry spark test shows very repeatable results, both in terms of energy (50-55 mJ) and discharge time. Individual dry spark waveforms in Fig. 5b are nearly identical. But, in the hot fire test (Fig. 5a), the waveforms are inconsistent. Spark 6, for example, almost appears to be quenched based on its short discharge time. However, its

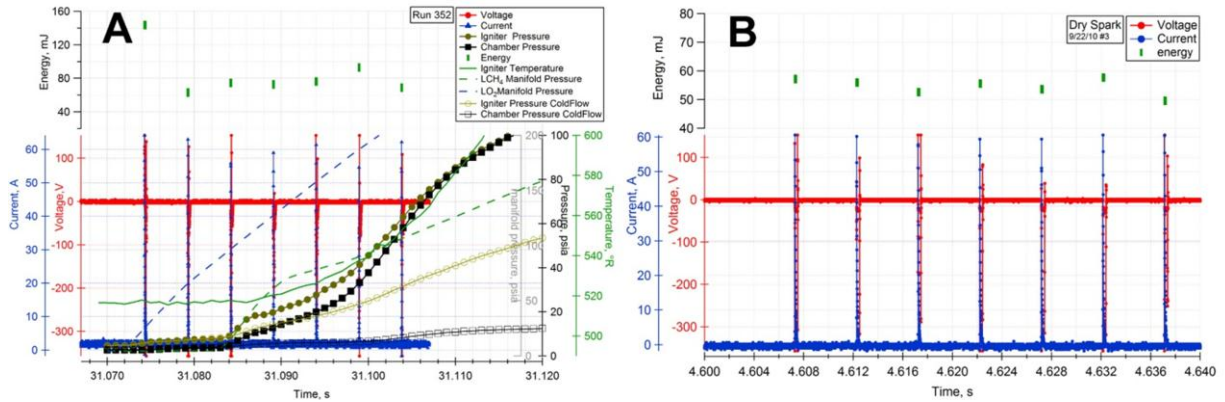


Figure 4: Example waveforms from the Unison exciter overlaid with the flow data. (a) A hot fire test indicates inconsistent spark behavior and (b) a dry spark test (no propellant flow so no pressure data) shows repeatable, consistent spark performance.

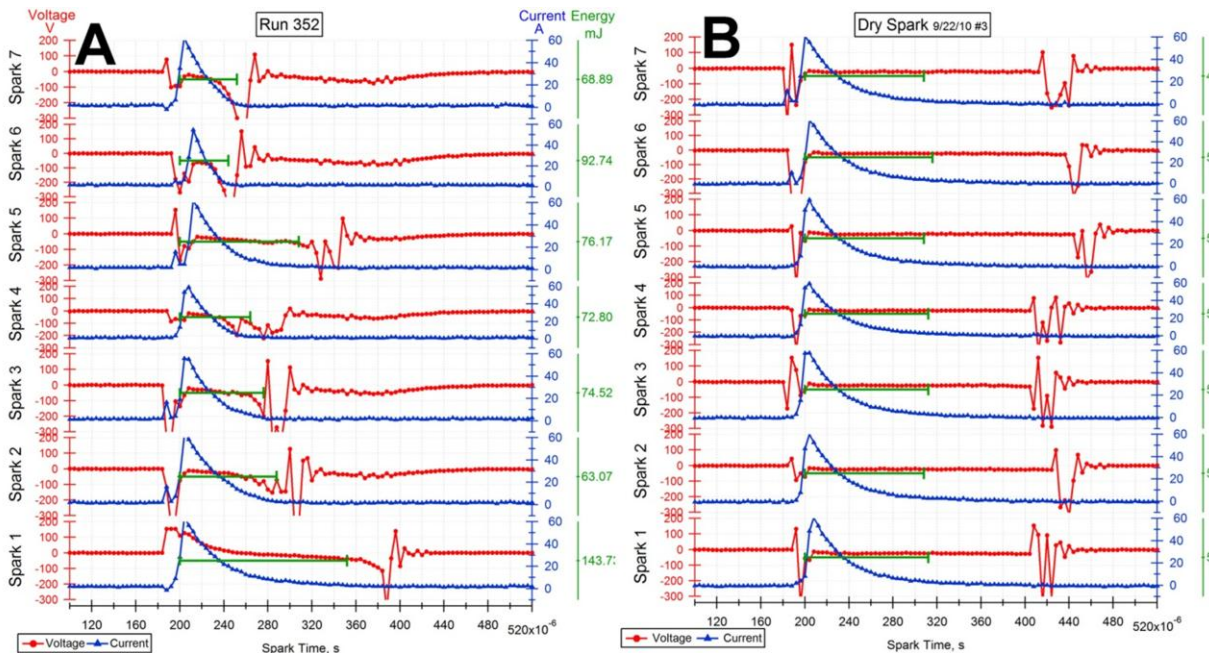


Figure 5: Close up plots of individual spark waveforms for the Unison exciter. (a) A hot fire run showing irregular behavior and (b) the repeatable waveforms of the dry spark data.

energy is quite high at 92 mJ whereas most of the others are around 60-75 mJ. This suggests that a full spark did occur, but with a higher than usual spark impedance resulting in a faster discharge.

The discharge results from the VEE show the same discrepancy between hot fire conditions and dry sparks. (Because of the similarity, these graphs are omitted from this document, but can be found in Ref. 10). However Fig. 3 does show a VEE spark train relative to flow conditions. On this time scale, the primary difference with VEE (versus the Unison) is the voltage signal waveform. For the first discharge in Fig. 3, the voltage has an “h” shape with the spike(s) representing the (<1 ms) spark discharge, while the gradual voltage decline (the hump of “h” shape) marks the capacitor recharge. The shape was evident in all the dry sparks for the VEE. However, none of the subsequent hot fire sparks in Fig. 3 show this pattern. The absence of capacitor recharging cycles and little to no spark discharge current indicates that the capacitor never fully discharged. These incomplete discharges tended to be most prominent later in the spark train, after ignition had occurred.

B. Spark Timing

The timing of the sparks relative to the flow conditions impacted both waveform characteristics and ignition probability. Figures 6 and 8 show this timing for the Unison exciter and VEE, respectively. The spark trains for all

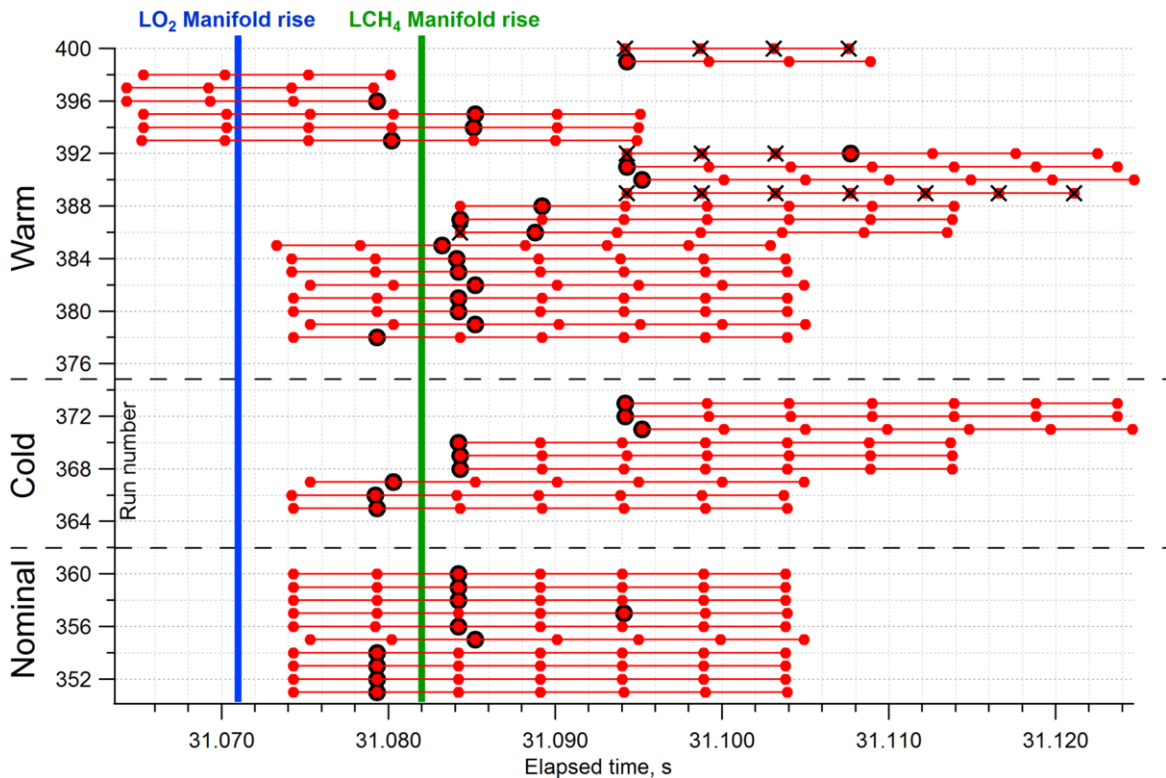


Figure 6: The Unison spark occurrences for each run are shown as a function of test time. Propellant flow initiation is indicated by vertical lines. Three propellant temperature conditions are represented. The ignition spark is circled. Dropped sparks are crossed.

the tests are plotted relative to the elapsed test time. The ignition sparks are circled. Dropped sparks (zero energy) are shown with a black “x”. The vertical lines represent pressure rise in the manifold, indicating propellant flow initiation.

For the Unison exciter (Fig. 6), the majority of igniting sparks occurred within ± 3 ms of methane flow introduction. Since oxygen is already flowing, this would be the earliest available combustible environment. Even though it appears that some sparks occurred in an oxygen only flow regime, this cannot be definitively proven within the uncertainties of the system response (± 3 -4ms). All ignitions, but one, were triggered off the spark that immediately preceded or followed the methane manifold pressure rise. Even when the spark command was delayed until 20 ms after the methane valve (runs 371-373) it was the first spark, thus the first one after methane flow introduction, that triggered ignition. The exception was run 357 which will be discussed later as a unique ignition event termed a “rumbling ignition”. Despite the system response uncertainty, a pattern emerges where the first tests of the day were ignited by the spark immediately prior to methane flow, while the latter tests were

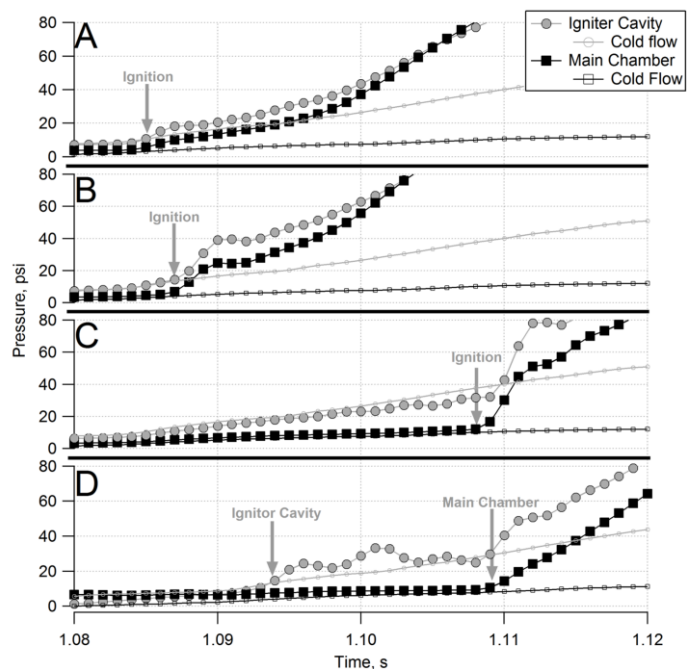


Figure 7: Ignition types are represented by the ignitor cavity pressure and chamber pressure traces. (a) Gradual, (b) Abrupt, (c) Late, and (d) Rumbling.

ignited by the spark immediately following methane flow. At the warm propellant condition, most ignitions were triggered immediately after the methane flow, despite earlier opportunities. Such behavior possibly hints at an ignition pattern relating to propellant temperature, with warmer propellants tending to correlate with slightly later ignition. The trend seems to hold in the nominal case, but spark command timing was changed after the third run of the cold propellant case, so this pattern could not be confirmed. However, it could be related to hardware temperature, which affects the injected propellant temperatures.

These timing shifts also affected the pressure rise behavior in the chamber and igniter cavity upon ignition. These are represented in Fig. 7, which shows the igniter cavity pressure and chamber pressure rise. The open symbols indicate the cold flow pressures, so deviation from this indicates an ignition event. Runs that ignited on the spark just prior to methane flow tended to have a ‘gradual’ ignition, as represented in Fig. 7a. The deviation from cold flow was marked by a gradual slope increase of the pressures in both the chamber and igniter cavity. Ignition occurring on the spark after methane flow resulted in an ‘abrupt’ ignition (Fig. 7b), where there was a sudden, sharp slope change in both pressure traces. ‘Late’ ignitions (Fig. 7c) were those that occurred at least 10 ms after fuel entry when the cold flow pressure was higher (generally when the igniter was intentionally activated late). The pressure spike was also more severe than for the abrupt ignition. The final scenario is a ‘rumbling’ ignition (Fig. 7d), which was an unusual case. In all other scenarios, the chamber and igniter cavity pressure departures are nearly simultaneous. However, in the rumbling ignition, igniter cavity pressure begins to deviate from cold flow while main chamber pressure continues to track its cold flow profile. This suggests a reaction in the igniter torch cavity, possibly an unstable flame kernel that did not immediately induce ignition of the main chamber. The rumbling ignition type only occurred once during this test series, but will be discussed later in reference to the previous I-bit test series.

For the VEE (Fig. 8), the sparks timed nearest to methane flow introduction also tended to favor ignition. There was more variability in ignition timing here (versus the Unison) because spark to spark energies were also varying. There were also more dropped sparks, which often occurred immediately after ignition. The ability to vary spark rate (Runs 313-326) was key in identifying the pressure response time relative to ignition, and thus the ignition spark.

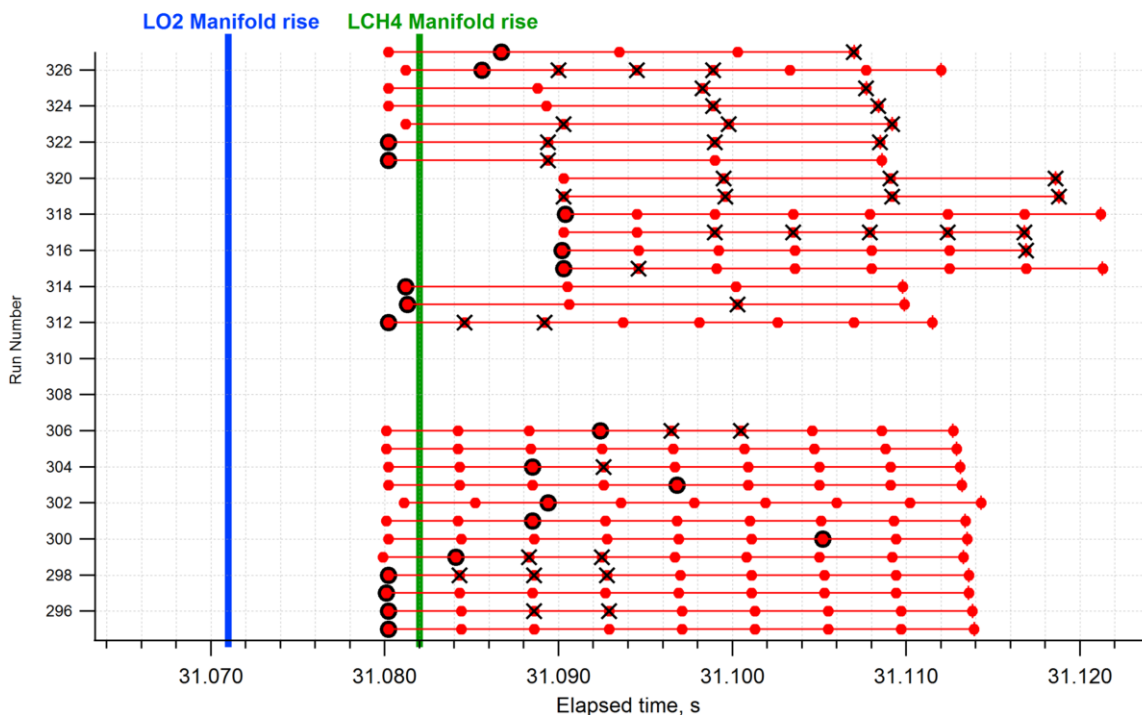


Figure 8: The VEE spark occurrences for each run as a function of test time. Vertical lines denote first indications of propellant flow. The ignition spark is circled, and dropped sparks are crossed out.

C. Energy

The variable energy exciter (VEE) was designed to have a tunable energy output. For dry spark conditions, the VEE generated consistent sparks of set energies from 30 to 50 mJ. However, under hot fire conditions, spark delivery behavior changed. Figure 9 shows VEE spark trains for a group of tests with the same spark rate, but different energy setpoints. The ignition sparks in each run are outlined. Inconsistency in spark behavior over the course of the spark train is evident. Overall, the spark energies appear to decrease later in the spark train. In several tests, this decrease seems to be triggered by the ignition spark. Also note that the igniting spark was not always the highest energy prior to ignition. Given the variability in the VEE's energy output, and a limited data set, it is difficult to draw any conclusions about spark energy effects on ignition probability.

In contrast, the Unison exciter was a fixed energy unit, but delivered more consistent spark energies. This is shown in Fig. 10, where tests are grouped by propellant temperature conditions. The dry spark energies are shown at each condition (thick black line) for reference. Many of the highest spark energies were not valid due to an overdrive effect on the Digital Oscilloscope Amplifier. This was most common on the first spark of the train for which the gap breakdown voltage (BDV) tended to be higher since there was no residual ionization from previous sparks. (BDV refers to the peak voltage achieved by the initial high voltage pulse before it ionizes the gases in the gap to create a spark). When large, the voltage spike frequently overdrove the DSO amplifier such that its slow recovery response caused a falsely high energy reading. (This artifact is apparent in Fig. 5a spark 1 by the slowly relaxing, inverted (positive) polarity of the spark voltage for the initial $\sim 1/3$ of the discharge. Given the uni-polar spark current output of the Unison exciter, an inverted (positive) polarity for spark voltage cannot be valid.)

These overdrive sparks are indicated by an "X" in Fig. 10, while the sparks that triggered ignition are circled. In many cases it was an overdrive spark that caused ignition. In fact, the frequency of this coincidence suggests that higher breakdown voltages and/or associated gap conditions may increase the ignition probability of a given spark. The energies in the cold and nominal cases were consistently higher than the dry spark baseline of 55 mJ, while the warm condition was similar to the dry spark. The data scatter is widest in the warm case, which may be due to the larger sample size (23 tests). Conversely, the energies were quite consistent at cold propellant conditions. There is a slight energy increase as the train proceeds, which is particularly noticeable in the nominal temperature case. This may be due to the higher pressure/flow conditions late in the spark train which drives up the spark impedance, and results in a higher energy transfer efficiency, and shorter spark duration.

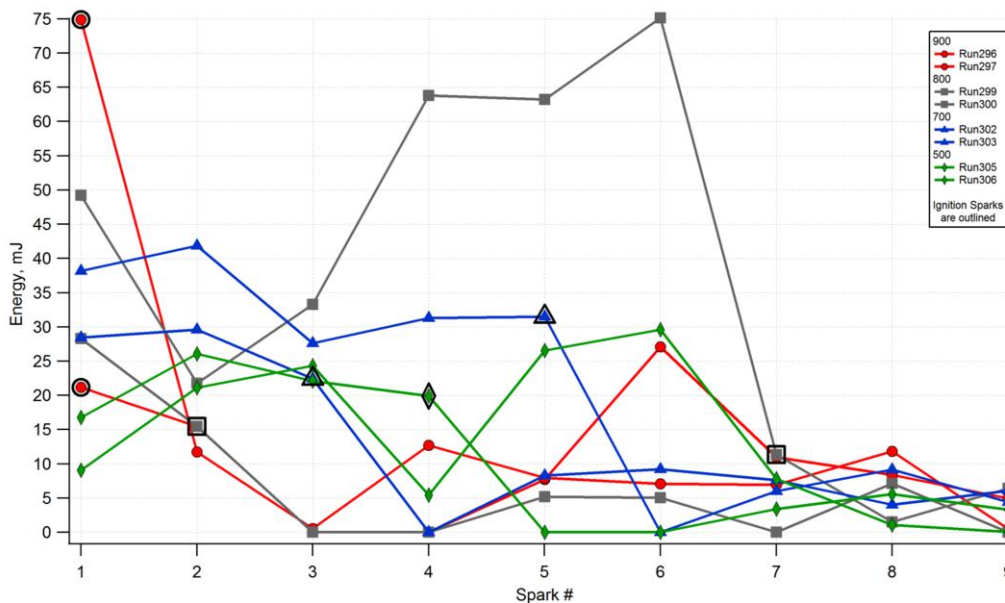


Figure 9: Spark energies are shown for a group of VEE tests at the same spark rate, but varying setpoint energy. Ignition sparks are outlined. The energies over the spark train vary widely, but appear to decrease late in the spark train, after ignition has occurred.

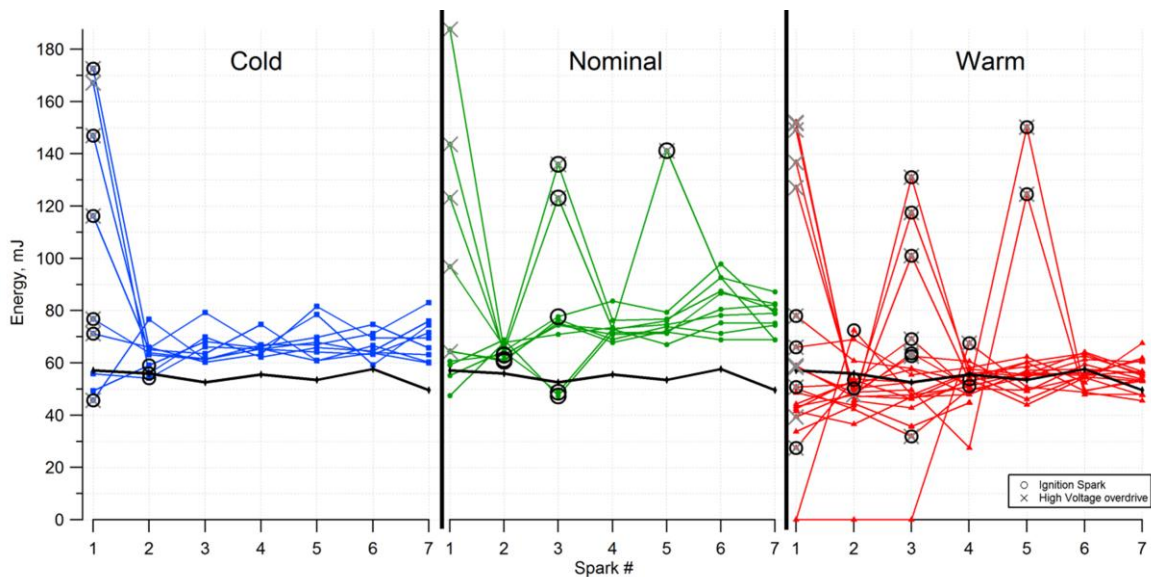


Figure 10: The spark energies for all Unison Exciter tests, grouped by propellant temperature conditions. The thick line represents the dry spark energies, which are consistent at ~55 mJ. The igniting spark for each run is circled. Energies which are suspect due to a high voltage overdrive issue are crossed out.

IV. Discussion

It was observed that the spark behavior in an engine environment was significantly different than the corresponding dry sparks (room air, no propellant flow). Both the VEE and Unison demonstrated repeatable spark waveforms in terms of discharge time, profile, and energy for dry spark tests. During hot fire engine tests, however, the waveforms and resulting energies were inconsistent within a single spark train. This indicates that the propellant flow field has a significant impact on spark behavior.

It has been noted in previous studies¹¹ that minimum ignition energy is higher in flowing mixtures due to a reduction in deposited energy density as the spark is stretched downstream. Likewise, previous experiments^{12,13} of ignition in turbulent premixed methane-air mixtures noted that the strain rate fluctuations at the spark location prevented stabilization of the flame kernel. For turbulent non-premixed flows, local mixture ratio fluctuations also affect ignitability near the spark. The randomness of these fluctuations causes ignition success to be probabilistic, so a higher spark energy is typically needed to ensure ignition.

Here, the flow effects are evident in the spark waveforms themselves, namely the spark discharge times. Figure 11 shows the average energy integration time for each spark over all VEE and Unison tests. In both cases, the discharge time decreased as the spark train proceeded. Since the spark train was applied coincident with the introduction and ramp up of propellant flow, this reduction in individual spark duration correlates with an increasing flow rate and pressure. This trend is more severe in the VEE, where ignition also seems to adversely impact spark behavior.

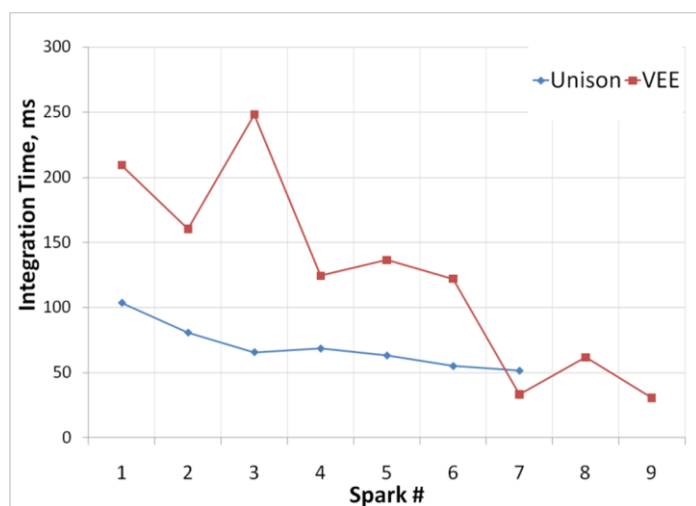


Figure 11: Average energy integration times indicate spark discharge time for the Unison and VEE.

These patterns of spark behavior may be primarily attributed to the effect of increasing pressure on spark discharge impedance and associated power dissipation (I^2R) for each discharge. Ultimately, there is a limit to an exciter's capability to drive higher impedance sparks. This is governed by the combination of its storage capacitor voltage and internal series inductance, referred to as "capacitor driving voltage". (This is distinct from the high voltage pulse and associated breakdown voltage, which triggers initial current across the spark gap). When exciter capacitor driving voltage is sufficient (as with Unison) to sustain higher voltage sparks, discharge of capacitor stored energy is faster and spark duration shorter. However, if exciter capacitor driving voltage is already marginal (as with VEE), then the higher spark voltage requirements prevent full discharge of capacitor and sparks get interrupted, or quenched. This tendency is exacerbated when the VEE's spark energy (capacitor voltage) is at a low setpoint.

Sparks timed after ignition with the VEE were also frequently either quenched (partially discharged) or dropped (not discharged). While these post-ignition sparks are not critical from a pure operations standpoint, they do reveal some fundamental behaviors. These ignition effects could also be attributed to an increased pressure environment caused by the flame kernel. However, another contributing factor could be flame induced ionization. The level of flame induced ionization is small compared to the ionization in the spark channels, so it is unlikely to significantly affect discharge impedance. However, it could be sufficient to reduce the voltage needed for gap breakdowns that initiate sparks. Due to the design of the VEE, this could allow a premature, reverse polarity breakdown during the transformer "charging" interval. During this period, ramping of current through the transformer primary generates a moderate, (~800 V) reverse polarity voltage on the transformer secondary (VEE output). If ambient ionization is sufficient, this reverse polarity voltage can cause a breakdown. The result is a short duration (~2 μ s), weak (<1 mJ) spark powered by collapse of the exciter output transformer's magnetic field, and not by a full capacitor discharge. It manifests as an apparent dropped spark for the data acquisition sample rates (1 sample/4 μ s) used here. Although this supposition might be argued to conflict with Paschen breakdown limits for the gap and pressures involved, the level of post-ignition ionization was likely sufficient to suppress or render invalid such limits. The presence of the flame induced ionization could be sufficient to counter the pressure increase induced either by flow ramp up or by the ignition flame kernel itself.

The few Unison spark dropouts all occurred prior to ignition, typically only in late spark application conditions (Fig. 6: Runs 386, 389, 392, and 400). By these times, pressure in the igniter cavity had risen to a level that rendered the cable-attenuated Unison HV pulses (~6 kV) marginal relative to the effective Paschen breakdown threshold^{14,15} for the gap. A similar explanation may apply to VEE dropped sparks that occurred late in instances of non-ignition (Fig. 8: Runs 317, 319, 320, 323-325). However, unlike the VEE, the pressure rise caused by ignition did not cause dropped sparks for the Unison. This suggests that the post-ignition ionization may have been sufficient to make the gap mildly conductive, facilitating breakdown at the higher pressures by lowering breakdown voltages substantially below Paschen curve levels. The Unison had a higher capacitor driving voltage, but lower HV pulse, than the VEE. So provided its lower HV pulse could achieve breakdown and thereby initiate each spark, it was able to sustain these sparks to completion despite their elevated discharge impedances caused by the ignition pressure rise.

Propellant temperature was only varied with the Unison exciter tests, making it difficult to draw conclusions regarding temperature effects from this tests series alone. It was observed that at the warm propellant condition most ignitions were triggered immediately after the methane flow (Fig. 6). Such behavior possibly hints at an ignition pattern relating to propellant temperature, with warmer propellants tending to correlate with slightly later ignition. The trend seems to hold in the nominal case, but could not be confirmed with cold propellant case. This could be related to hardware temperature, which affects the injected propellant temperatures. The effect is more clear in the pulse strings (sequential short engine burns) of I-bit testing⁷. In those tests propellant temperature did exhibit a distinct effect on ignition behavior, especially in regard to the incidence of rumbling ignition.

This ignition test series was performed as a series of single-shot hot fire runs where a warm nitrogen purge through engine manifolds and igniter was maintained between each engine firing. This kept the hardware at relatively warm temperatures (~480-500 °R) prior to each run, effectively resetting hardware conditions and ensuring gas phase propellant in the igniter cavity. In contrast, pulse strings in the I-bit test series were commanded without intervening purge cycles. Igniter hardware was able to chill-in with continuous propellant flow as each pulse string progressed. Thus allowing the hardware to achieve temperatures more comparable to the propellants, permitting the possibility of liquid, or mixed-phase, propellant injection into the igniter. Consequent changes of ignition behavior that occurred during the progression of each pulse string could thereby have been triggered by the developing spray injection and/or associated MR fluctuations.

These ignition behavior transitions are evident in Fig. 12 which shows ignitions for 20 sequential pulses at nominal propellant conditions. The igniter cavity pressure traces for each pulse are plotted against a relative time scale in milliseconds. Cold flow pressure is also shown as the solid line. Figure 12a shows the first 6 pulses. The first pulse was a stable, gradual ignition but the next three pulses showed fluctuations in the igniter cavity, indicative

of a rumbling ignition. The behavior then began to stabilize as abrupt ignitions for pulses 7 -12, shown Fig. 12b. The last 6 pulses, Fig. 12c show very repeatable abrupt ignitions. The transition from gradual ignition early in the test to abrupt ignition late for a pulse train in the I-bit test series exhibits the same trend observed for ignition tests over the course of a test day (Fig. 6).

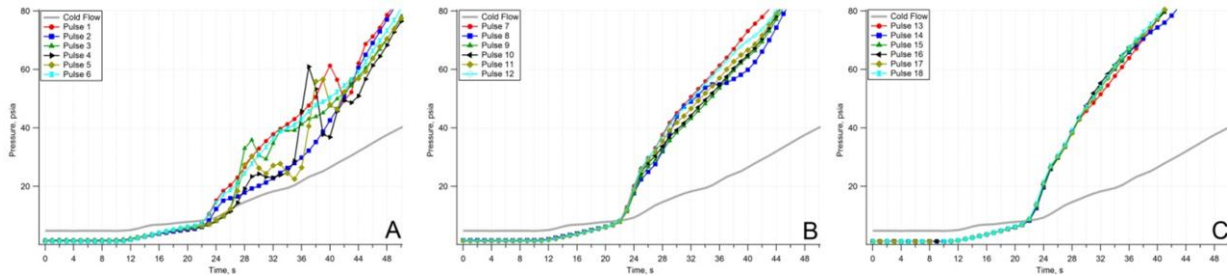


Figure 12: These three images show the igniter pressures from 18 consecutive pulses. The first 6 pulses in (a) have fluctuations indicative of a rumbling ignition. In (b) the behavior becomes more consistent, culminating in very repeatable abrupt ignitions by the last 6 pulses in (c).

In terms of minimum ignition energy, the lowest observed ignition was ~ 1 mJ with the VEE (Run 318). This suggests that a well-timed spark, even at low energy, can trigger ignition. However, the mix of ignitions and non-ignitions for similarly timed 1-6 mJ VEE sparks indicates that ignition for these low energy sparks is not reliable. Other studies involving turbulent and/or non-premixed flows have noted a similar probabilistic nature with regard to minimum ignition energy¹². The number of tests needed to quantify such probabilities could not be accomplished within the PCAD test program. While the Unison exciter did not permit energy variation, it was able to reliably ignite the flow. The majority of sparks occurred at or above the dry spark baseline of 55 mJ. The timing of the sparks was critical; the only failed ignitions occurred when sparks were limited to an interval before Methane flow (Runs 397 & 398) or delayed until after igniter pressure exceeded a level corresponding to Paschen breakdown constraints (Runs 389 & 400).

V. Conclusion

The ignition margin test series was performed at NASA Glenn Research Center's altitude combustion stand using the 100 lb_f LO₂/LCH₄ RCE. With the goal of exploring minimum energy requirements for this propellant combination, a total of three exciters were tested, two of which were presented here. All were instrumented with a high-speed digital oscilloscope to resolve current and voltage waveforms of the spark discharges. These data were synchronized with the engine pressure and temperature data to enable identification of the ignition spark.

For all exciter units, spark waveforms in the hot fire, engine environment differed from those of dry spark tests (room condition, no-flow environment). The dry sparks demonstrated repeatable waveforms and consistent spark energies; whereas the hot fire tests had changing waveforms and inconsistent energies within a single spark train. As igniter pressure and flow rate increased during progression of each spark train, spark discharge voltages tended to increase and result in shorter spark durations. This indicates that rising pressures and flow rates substantially increase spark impedance, which, at some point, can compromise an exciter's ability to complete sparks without quenching. That is, higher pressures and cross-flows in the spark gap region can raise spark voltage to levels that exceed the limit that a particular exciter can tolerate. If spark voltages reach exciter limits, premature extinctions and/or reductions of spark energy (i.e., quenched sparks) typically result. If these features occur prior to ignition, this has an adverse impact on ignition promptness and reliability.

After ignition, the accelerated pressure rise caused by the flame kernel had the most obvious effect on spark discharge characteristics. The VEE, which had a higher (9-10 kV) HV pulse, was able to achieve breakdown and initiate sparks at elevated pressures, but its low capacitor driving voltage was often unable to sustain, or complete each spark. Sparks occurring after ignition therefore tended to quench. This was not the case for the Unison which, with its higher capacitor driving voltage, always delivered full sparks after ignition. It might be surprising that the Unison's lower HV pulse (6 kV) was sufficient to obtain breakdown in the higher post-ignition pressure environment. However, this may be attributed to ignition induced flame ionization which facilitated reduced BDVs, effectively invalidating Paschen-law pressure effects. By this same mechanism, flame ionization may have caused some post-ignition dropped sparks for the VEE, due to its circuit design.

The Variable Energy Exciter (VEE) was designed to allow precise control and variation of spark energy so that ignition energy limits could be determined. However, the engine environment caused a great deal of variability in waveform behavior and delivered energies. The unit's energy adjustment only served to limit the overall range of

spark energies, but the sparks themselves were not repeatable, primarily due to erratic spark quenches. The individual sparks that triggered ignition were identified, but also exhibited a large scatter in energies. In some cases ignition was triggered by quenched sparks of energies as low as 1-6 mJ, although ignition by such sparks (in same time interval) was not reliable. By comparison, similarly timed, higher energy Unison sparks (55-75 mJ) regularly yielded ignition.

Ignition probability depends not just on spark energy, but also on spark timing relative to propellant flow introduction. A sequence of several sparks over an appropriate time interval is required such that their cumulative probability of ignition approaches 100 percent. The spark timed nearest to the initiation of propellant flow (either immediately before or after) tended to trigger ignition. A high spark rate in this region would increase ignition probability.

This ignition timing also impacted the nature of the ignition, as indicated by the pressure behavior in the igniter cavity and chamber. Ignitions in warmer propellant conditions tended to have a gradual pressure rise, while the colder temperature tended toward a more severe pressure rise. This was supported by data from the previous test series which examined engine performance in pulsed mode operation, where temperature variation effects could be examined over the course of a pulse train. In the unique case of a 'rumbling' ignition, which was primarily observed during pulse testing, the chamber pressure was unaffected by pressure fluctuations in the igniter cavity. In most cases, pressure response in the igniter cavity and chamber were simultaneous. The rumbling ignition suggests that an unstable flame kernel can develop in the igniter cavity. However, all rumbling ignitions did ultimately trigger main chamber ignition, albeit delayed.

From the standpoint of future LO₂/LCH₄ engine design, these RCE tests have demonstrated that reliable ignition of the propellants is possible. While spark energy was found to exhibit a significant influence on this reliability, no distinct minimum spark energy for reliable ignition was found. Rather, ignition displayed a stochastic dependence on delivered spark energy. For the dynamic engine environment, delivered spark energy did not always correspond to the rated output spark energy of the exciter. It is therefore important to verify that exciter design characteristics, such as HV pulse and capacitor driving voltage, are sufficient to guarantee un-quenched spark delivery under actual igniter conditions. While higher spark energies tend to increase ignition probability, spark timing and repetition rate also play a critical role. Lower energy sparks that are well timed with respect to propellant entry can achieve ignition. Observations indicate that sparks early in the flow ramp-up have the highest probability of success. Several sparks over the optimum time interval appear to be necessary to ensure an adequate cumulative probability of ignition. Thus, a high spark rate (here, 200-300 sps) yielding more sparks in this optimum interval helps facilitate ignition reliability. Later sparks, timed after the optimum interval, can still trigger ignition, but do so with reduced probability.

Acknowledgments

The authors appreciate the efforts of the facilities team which operated the ACS facility and made testing possible. This work was supported by the Propulsion and Cryogenic Advanced Development (PCAD) project with which was part of the former NASA Exploration and Technology Development Program (ETDP).

References

- ¹Melcher, J.C. and Allred, J.K., "Liquid Oxygen/Liquid Methane Testing of the RS-18 at NASA White Sands Test Facility", AIAA 2008--4843, 44th AIAA/ASME/SAE/ASEE Joint Propulsion Conference and Exhibit, Hartford, CT, July 21--23, 2008.
- ²Melcher, J.C. and Allred, J.K., "Liquid Oxygen/Liquid Methane Test Results of the RS-18 Lunar Ascent Engine at Simulated Altitude Conditions at NASA White Sands Test Facility", AIAA 2009--4949, 45th AIAA/ASME/SAE/ASEE Joint Propulsion Conference and Exhibit, Denver, CO, August 2-5, 2009
- ³Stone, R., Tiliakos, N., Balepin, V., Tsai, C.-Y., and Engers, R., "Altitude Testing of LOX-Methane Rocket Engines at ATK GASL", AIAA 2008-3701, 26th AIAA Aerodynamics Measurement Technology and Ground Testing Conference, Seattle, WA, June 23-26, 2008.
- ⁴Robinson, P.J., Veith, E.M., Hurlbert, E.A., Jimenez, R., and Smith, T.D., "100-lbf LO₂/LCH₄ - Reaction Control Engine Technology Development for Future Space Vehicles", 59th International Astronautical Federation, Glasgow, Scotland, United Kingdom, September 29 - October 3, 2008.
- ⁵Marshall, W.M. and Kleinhenz, J.E., "Performance Analysis of Duration Tests of a 100 lbf LO₂/LCH₄ Reaction Control Engine at Altitude Conditions at NASA Glenn Research Center", NASA/TM-2011-217131.
- ⁶Marshall, W.M. and Kleinhenz, J.E., "Hot-Fire Testing of 100 lbf LOX/LCH₄ Reaction Control Engine at Altitude Conditions", JANNAF 57th JPM/7th MSS/5th LPS/4th SPS Joint Subcommittee Meeting, Colorado Springs, CO, May 3-7, 2010.
- ⁷Marshall, W.M. and Kleinhenz, J.E., "Analysis of 100 lbf LO₂/LCH₄ Reaction Control Engine Impulse Bit Performance at Altitude Conditions," NASA TM-2012-217613, 2012.

- ⁸Lawver, B.R. and Rousar, D.C., "Ignition Characterization of the GOX/Ethanol Propellant Combinations", AIAA-84-1467. 1984
- ⁹Lawver, B.R., Rousar, D.C., and Wong, K.Y., "Ignition Characterization of LOX/Hydrocarbon Propellants", Contract NAS9-16639, Aerojet TechSystems Co., NASA CR-171884, 1985.
- ¹⁰Kleinhenz, J.E., Sarmiento, C.J., and Marshall, W.M., "Experimental Investigation of Augmented Spark Ignition of a LO₂/LCH₄ Reaction Control Engine at Altitude Conditions," NASA TM-2012-217611, 2012.
- ¹¹Glassman, I. Combustion. 3rd Edition. Academic Press. 1996. (pg 347)
- ¹²Mastorakos, E. "Ignition of turbulent non-premixed flames", Progress in Energy and Combustion Science, 35:57-97, 2009.
- ¹³Huang, Shy, Liu, Yan, "A transition on minimum ignition energy for lean turbulent methane combustion in flamelet and distributed regimes", Proceedings of Combustion Institute. 2007; 31:1401-9
- ¹⁴Bury, K.M. and Kerslake, T.W. "The effect of Reactor Control System Thruster Plume Impingement on Orion Service Module Solar Array Power Production". NASA-TM-2008-215423. 2008
- ¹⁵Devins, J.C. and Crowe, R.W. "Electric Strength of Saturated Hydrocarbon Gases". Journal of Chemical Physics, Volume 25-5, pp 1053-1058. 1956.